Oncology
and Radiotherapy ©

17 (11) 2023: 001-011 • RESEARCH ARTICLE

Synthesis, characterization and cytotoxic activity study of Mn (II), Co (II), and metal complexes with new schiff base against the hepatocellular carcinoma (SK-GT-4) cancer cell

Zaid N. O. Al-Husseini, Jasim M. S. Alshawi
Chemistry Department, College of Education for Pure Sciences, Basrah University, Basrah, Iraq.

ABSTRACT

This paper involved the synthesis of a new compound by condensing O-Phenylenediamine (OPD) and 4-Methyl-o-phenylenediamine with pyrrole-2-carboxaldehyde through a condensation reaction. Following that, transition metal complexes of Mn (II) and Co (II) were prepared by reacting the respective metal chlorides with the ligand in a 1:1 molar ratio. To characterize the ligand and its metal complexes, a comprehensive range of spectroscopic and analytical techniques was employed, confirming their tetrahedral geometry. Additionally, the researchers investigated the potential cytotoxic effects of hepatic cells cancer (SK-GT-4) cancer cells treated with the Schiff bases and its metal compounds.

Key words: 2-Formylpyrrole, 4-Methyl-o-phenylenediamine, cancer cell, SK-GT-4, Cytotoxic Activity, cancer cells, schiff base

Address for correspondence:

Zaid N. O. Al-husseini, Chemistry Department, College of Education for Pure Sciences, Basrah University, Basrah, Iraq. E-mail: noorzaid297@gmail.com

Word count: 4110 **Tables:** 5 **Figures:** 21 **References:** 30

Received: 06 September, 2023, Manuscript No. OAR-23-113949
Editor assigned: 08 October, 2023, Pre-QC No. OAR-23-113949 (PQ)
Reviewed: 03 November, 2023, QC No. OAR-23-113949 (Q)
Revised: 16 November, 2023, Manuscript No. OAR-23-113949 (R)
Published: 30 November, 2023, Invoice No. J-113949

INTRODUCTION

Schiff bases are extensively studied and considered highly important due to their wide range of biological applications, ease of preparation, chelating properties, and stability [1,2]. These ligands have contributed significantly to the field of inorganic biochemistry and have shown pharmacological activities such as antibacterial effects [3], antioxidant properties [4,5], anticancer potential [6], and antifungal properties [7]. Biological, analytical, and pharmaceutical uses of Schiff bases produced by 3,4-diamino the benzophenone and its complexes have all been explored.

Numerous studies have explored their uses, such as antimicrobial and molecular docking studies, as well as investigations into the thermodynamics of complex formation with metal ions [8,9]. In our current research, we synthesized four new ligands by reacting o-phenylenediamine and thiophene-2-carboxaldehyde in ethanol as a solvent. We then formed metal complexes with selected metal ions. All the complexes exhibited tetra-coordinated metal centers with paramagnetic properties and sp3 hybridization. These results prompted us to look into the potential therapeutic effects of complexes of the guanidine as ligand on a hep cell cancer (SK-GT-4) cell line.

MATERIALS AND METHODS

Chemicals were sourced from Merck, BDH, and Sigma-Aldrich without the need for additional purification. The ligand and its complexes were analysed for their melting points using model 9300. For the 1HNMR spectroscopy, DMSO-d6 was the solvent of choice and a Varian 500MHz Spectrophotometer was employed. Mass Spectra were obtained with a Shimadzu Agilent Technologies 5975C instrument, and UV-Visible spectra were recorded using a Shimadzu double band model 1700 spectrophotometer. Magnetic susceptibility measurements were carried out using a Faraday method on a balance magnetic MSB-MKI instrument.

with diamagnetic corrections made according to Pascal's constants. IR spectra were obtained using a Shimadzu FTIR 8400 spectrometer, utilizing KBr pellets within the wavelength

range of 4000-400 cm-1. For toxicological studies, various equipment and supplies were used, including an Autoclave from Arnold Sons, USA, a biohazard safety cabinet from Germany, a centrifuge from Hermle, Germany, a cooling centrifuge (Beckman Model J2-21) from the USA, a deep freezer (-80°C) from Marubeni, Japan, a distillatory apparatus from Ogawa Seiki, Japan, a drying and sterilizing oven from Hermle, Germany, an ELISA reader from Organon Teknika in Beelchum, an incubator from Memmert, Germany, an inverted microscope from Leica, Germany, multiwall plates and 96-well Lab-TeK and Nunc plates from the USA, a 0.22 µm Millipore filter from Sartorius, Germany, a pH meter from LKB, Sweden, sterile 25 and 75 cm2 tissue culture flasks from Nunc, Denmark, a vacuum pump from Leitz, Germany, and a water bath from Memmert, Germany.

Synthesis of schiff base (A)

To carry out the synthesis described in Figure 1, Pyrrole-2-carboxaldehyde (0.951 g, 0.01 mol) (about 4 to 5) drops of glacier acetic acid were included in a solution of which was dispersed in 10 mL liquid ethanol.. Separately, o-phenylenediamine (0.540 g, 0.005 mol) was dissolved in 25 mL of ethanol. The solution of o-phenylenediamine was then slowly added to the aldehyde solution while the mixture was refluxed. The refluxing process was continued for 20 hours. After refluxing, the mixture was filtered, and the resulting product was subjected to recrystallization using ethanol.

Synthesis of schiff base (B)

To perform the synthesis described in Scheme 1, Pyrrole-2-carboxaldehyde (0.951 g, 0.01 mol) was mixed wih 4 to 5 drops of glacier acetic acid and placed in 10 mL of ethanol. Separately, 4-Methyl-o-phenylenediamine (0.610 g, 0.005 MOL) was mixed with 25 ML of alcohol. The solution of 4-Methyl-o-phenylenediamine was then gradually added to the aldehyde solution under reflux. The refluxing process was carried out for 20 hours. After completion, the mixture was filtered, and the resulting product was subjected to recrystallization using ethanol.

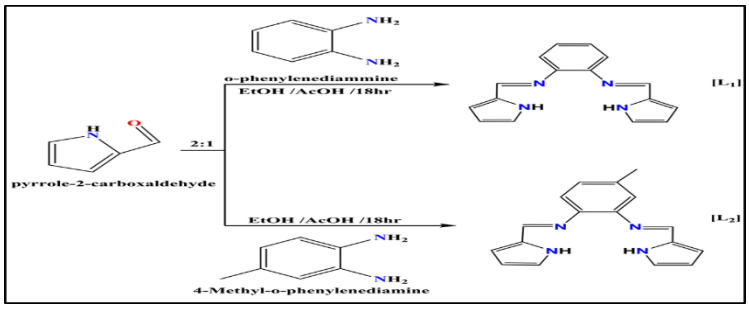

Fig 1. Synthesis of Ligand Schiff base (A)and(B)

Preparation of metal complexes

To prepare the (1:1) chelate complexes between the metal and the ligand, a solution of the Schiff base (0.002 mol) in 25 ml of hot ethanol was prepared. In a separate step, the corresponding hydrated metal chloride salts, MnCl2.2H2O and CoCl2.6H2O (both 0.002 mol), was mixed with 25 ML of hot ethanol. The hot ethanol solution of the ligand was then mixed with the hot ethanol solution of the metal chloride salts. The resulting mixture was refluxed on a water bath for a duration of 3 hours. Upon cooling, the complexes precipitated out of the solution (as shown in Scheme 2). The The complexes obtained were separated by filtration, followed by washing with ethanol and drying under vacuum. The physical properties and analytical data for these complexes can be found in Table 1, as referenced by sources [10,11].

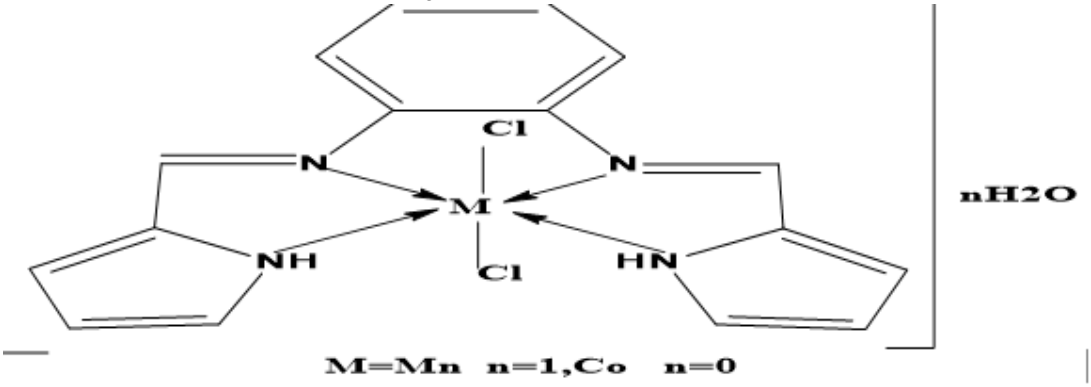

Fig 2. Synthesis of metal complexes (MnA)and(CoA)

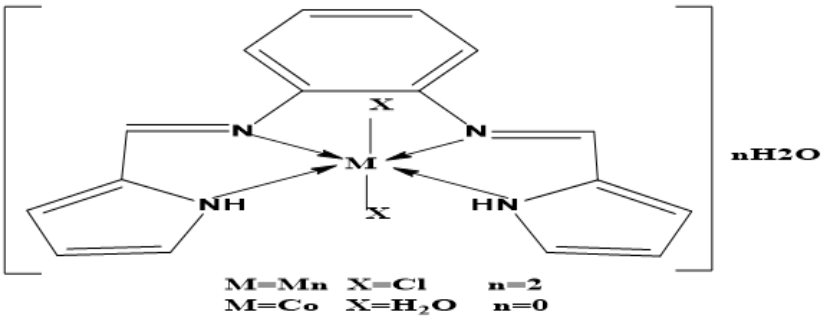

Fig 2. Synthesis of metal complexes (MnB) and (CoB)

Biological activity

The cytotoxicity of the Schiff bases and their complexes was assessed using the MTT assay after a 72-hour incubation period against the SK-GT-4 cell line, which is a type of esophageal cancer. The results revealed significant activity of certain compounds against SK-GT-4 cells, particularly the complexes of Mn (II) with Schiff bases L A and L B at varying concentrations. These compounds underwent biological and toxicological tests on normal cells as well. Remarkably, both complexes exhibited a remarkable selectivity in targeting and killing cancer cells while sparing healthy cells. This makes them promising candidates for the treatment of skin cancer and retinal cancer, as they demonstrate exceptional selectivity and effectiveness [12].

RESULT AND DISCUSSION

The data presented in Table 1, along with the spectral information in Tables 2 and 3, provide evidence for the successful synthesis of ligands L(A,B) through the condensation reaction between o-phenylenediamine and Pyrrole-2-carboxaldehyde as shown in Scheme 1. The designed complexes 1-4 were prepared with a 1:1 stoichiometric ratio of ligand to metal. The results obtained from various analytical techniques support the conclusion that the metal complexes 1-4 can be represented by the general formula [ML]Cl2.

Tab 1. Characteristics of (LA), (LB), & their associated complexes

M.Wt	Colour	M.F	Yield %	M.P °C	Comp. No.
262.32	Brown, Coffee	$C_{16}H_{14}N_4$	71	174-176	LA
276.34	Dark Brown	$C_{17}H_{16}N_4$	72	150-152	LB
405.32	Brown	[Mn ($C_{16}H_{14}N_4$) Cl_2].H_2O	73	160-162	MnLA
389.32	Dark Brown	[Co ($C_{16}H_{14}N_4$) Cl_2]	69	250-252	CoLA
437.34	Dark Brown	[Mn ($C_{17}H_{16}N_4$) Cl_2].$2H_2O$	78	195-197	MnLB
396.34	Dark Olive	[Co ($C_{17}H_{16}N_4$)$2H_2O$]	84	80-82	CoLB

Mass Spectrum of Schiff base ligand

The mass spectrum of Schiff base ligand LA was analyzed, revealing several fragments with different mass-to-charge ratios (m/z) and relative abundances. The peak at m/z 262.1 corresponded to the intact Schiff base ligand molecule, confirming its molecular structure. Other notable fragments included m/z 234.1 and 209.1, corresponding to C15H12N3 and C13H11N3, respectively. Additionally, fragments at m/z* 183.1 and 91.13 were attributed to C11H9N and C6H5N. Figure 1 highlights these findings by drawing attention to the mass spectra and fragment pattern of the Schiff base ligand LA.s. Similarly, the mass spectrum of Schiff base ligand LB was also examined, demonstrating various fragments with distinct m/z values and relative abundances. The peak at m/z 276.1 corresponded to the intact Schiff base ligand molecule, further confirming its molecular structure. Noteworthy fragments included m/z 248.2 and 224.2, corresponding to C16H14N3 and C14H14N3, respectively. Additionally, fragments at m/z* 197.2 and 105.07 were attributed to C12H11N3 and C7H7N. Figure 2 shows the fragmentation pattern and mass spectra of the Schiff base ligand LB to support these conclusions [13].

^{1}H NMR Spectra

The 1H-NMR spectra of ligand LA, measured in DMSO-d6 as the solvent, revealed several distinct chemical shifts, as demonstrated in Figure 3. The NH group proton exhibited a singlet signal at 11.80 ppm, while the azomethine proton (CH=N) was observed at 11.00 ppm. Multiple signals between 7.60-5.50 ppm indicated the presence of aromatic protons [13]. Similarly, in the 1H-NMR spectrum of ligand LB, also measured in DMSO-d6 as the solvent and depicted in Figure 4, similar characteristic chemical shifts were observed. The NH group proton exhibited a singlet signal at 11.75 ppm, while the azomethine proton (CH=N) was observed at 10.50 ppm.

Multiple signals between 7.50-5.50 ppm indicated the presence of aromatic protons, and the CH3 group was represented by an emission at 2.45 ppm [14].

FT-IR Spectra

Figures 5-10 illustrate the IR spectra of Schiff base compounds LA and LB, as well as their complexes. These spectra demonstrate the absorption regions that are characteristic of the prepared Schiff base ligands. Specifically, the Schiff bases exhibit absorption bands in the infrared spectrum within the range of 1587-1645 cm-1, It may be explained by the C=N bond's stretching vibration. They also exhibit bands in the range of 3334-3450 cm-1, corresponding to the stretching vibration of the NH bond. Additionally, strong absorption bands within the range of 1420-1487 cm-1 indicate the stretching vibration of the C=C bonds in the aromatic rings. Furthermore, all the prepared Schiff bases display bands in the range of 3105-3238 cm-1, indicating the stretching vibration of the C-H bonds in the aromatic groups, and a band in the range of 2723-2755 cm-1, representing the stretching vibration of the C-H bonds in the aliphatic groups.

The metal complexes exhibit new bands around 709-748 cm-1 and 435-586 cm-1, which arise from the formation of M-N and M-NH bonds, respectively [15-17].

Tab 2. The FT-IR spectral data (cm-1) for the Schiff base ligand and its complexes.

Sym.	ᵛC-H(Ar)	ᵛC-H(alip)	ᵛC=N	ᵛC=C-(Ar)	ᵛN-H	ᵛC-N-	ᵛM-N-	ν (M-NH)	ᵛ(H_2O)
LA	3113	------	1645	1458	3388-3334	1350	------	------	
LB	3125	2920	1643	1400	3245	1352	----		
LAMn	3199	----	1635	1458	-----	1395	740	555	3211
LACo	3238	------	1636	1465	-----	1411	748	586	
LBMn	3194	2950	1638	1404	------	1309	709	542	3506
LBCo	3105	3120	1637	1406	------	1327	727	435	3427

Molar conductivity measurements

Table 3 presents the conductivity values (Λμ) of the prepared complexes dissolved in ethanol solvent at a concentration of 10-3M and at room temperature. The results indicate molar conductance values ranging from 18.1 to 9.3 S.cm2.mol-1, suggesting that the compounds are non-electrolytes [18]. However, the molar conductance of the LACO complex is measured at 29 S.cm2.mol-1, indicating its electrolytic nature. The presence of chloride ions outside the coordination sphere is indicated by this observation, as mentioned in reference [19].

Magnetic properties

According to Table 3, which summarizes data from sources [20-23], analyses of the magnetic characteristics of the synthesized complexes revealed that both Mn(II) & Co(II) compounds are electromagnetic and possessed a tetrahedral shape. The complex's effective magnetic moment (μeff) was computed using the following formulas: -

$$X_m = X_g . M.wt \ldots\ldots\ldots\ldots 1$$

$$X_A = X_m + D \ldots\ldots\ldots\ldots 2$$

$$\mu eff = 2.828 \sqrt{XA.T\ B.M} \ldots\ldots\ldots\ldots$$

Electronic Spectra

Table 3 presents information on the free ligands' UV-Vis spectrum LA and LB, as well as all the metal complexes. In the UV-Vis spectrum of ligand LA [24] shown in Figure 11, three peaks are observed at 218 nm, the π – π* and n – π* electronic transitions are associated with the wavelengths of 280 nm and 414 nm, respectively. In contrast, Figure 12 shows the electronic spectra of ligand LB [25], which has two peaks at 280 nm and 310 nm due to the * and n * electronic transitions.

The Electronic Spectra of Complexes

[Mn(LA)] Cl2:-The complex (Fig.13) showed absorption peaks at 535nm due to charge transfer(C.T) . which is a good evidence for square pyramidal geometry about Mn(II).

[Co(LA)]Cl2:-The complex(Fig-14) gave two peaks at 442nm and at457nm were found to be caused by (d-d) electronic transition type 4T1g → 4A2g(P) and 4T1g → 4A2g(F) suggesting octahedral geometry about Co(II) [26]

[Mn(LB)] Cl2:-The complex (Fig-15) showed absorption peaks at 522 nm due to charge transfer(C.T) . which is a good evidence for square pyramidal geometry about Mn(II).

[Co(LB)]Cl2:-The complex(Fig-16) gave two absorptions at 444nm assigned to charge transfer (C.T). suggesting octahedral.

Tab 3. Conductivity, magnetic moment, and electronic spectra of ligands and their complexes.

μeff (B.M)	Conductivity S.cm2.mol -1	Transition	Absorption bands(nm)	Compound
----	----	π →π*	205	LA
		π →π*	310	
		n →π*	392	
----	----	π →π*	260	LB
		n →π*	320	
5.08	11.4	π →π*	250	LAMn
		π →π*	310	
		MLC.T	386	
		^{6}A1g→^{4}T1g(P)	455	
3.44	16	π →π*	**292**	LACo
		n →π*	**371**	
		MLCT	**403**	
		4T1g(F)→4T1g (P)	**536**	
		4T1g(F)→ 4A2g(F)	**563**	
		4T1g(F)→ 4T2g(F)	**621**	
5.54	18.1	π →π*	2550	LBMn
		n →π*	315	
		A1g→4T1g (P)$_6$))	453	
		A1g→4T2g(G)$_6$))	549	
		A1g→4T1g(G)$_6$))	609	
4.3	9.3	π →π*	295	LBCo
		*π→ n	345	
		MLCT	382	
		(T1g(F) → 4T1g(P4))	573	
		(T1g(F) → 4A2g(F4))	624	

Thermogravimetry (TG), which is a thermal analysis technique, was utilized to examine the interaction between the metal and ligand as well as to investigate the thermal behavior and decomposition of the transition metal complexes. The complexes were subjected to thermogravimetric analysis under a controlled nitrogen atmosphere.The analysis started from room temperature and continued up to 600 ˚C, with a heating rate of 10 ˚C/min [27].

Thermal degradation of LB

The decomposition of LB occurred in two stages. The first stage showed weight loss peaks between 150-200 ˚C, indicating the breakdown of (CH3) with a calculated weight loss of 0.46 mg (5.84%). In the second stage, weight loss was observed in range of temperatures 210-350 ˚C, a sign of the demise of ($C_7H_{12}N$) with a calculated weight loss of 3.13mg (40%) (Figure 17).

Thermal degradation of Mn LB

The decomposition of Mn LB occurred in two stages. The first stage showed weight loss peaks between 130-220 ˚C, indicating the breakdown of (CH4) with a calculated weight loss of 4.08 mg (61.29%). In the second stage, weight loss was observed in range of temperatures 230-490 ˚C, a sign of the demise of (C6H9NCl) with a calculated weight loss of 2.66 mg (40%) (Figure 18).

Thermal degradation of Co LA

The thermal decomposition of Co LA occurred in four stages. The first stage showed weight loss peaks at 130-150 oC, indicating the decomposition of (CH6) with a calculated weight loss of 0.36 mg (4.57%). There was a weight decrease of in the second stage. (C2H2N) with a calculated weight loss of 0.94 mg (12%) within the range of 180 to 240 degrees . The third stage exhibited a weight loss of (C3H2N) with a calculated weight loss of 1.25 mg (16%) within the temperature range of 320-360 ˚C. Finally, (C5H2N) lost weight during the fourth stage. with a

calculated weight loss of 1.72 mg (22%) within the temperature range of 365-420 °C. These results were shown in Figure 19.

Kinetic and thermodynamic data analysis

The thermal decomposition of the complexes was analyzed using the Coats-Redfern method (1), and a Table 4 gives an outline of how the combinations behave when it comes to heat.

$$\frac{\log \frac{W_f - w_t}{T^2}}{} - \log\left[\frac{AR}{\theta E}1 - \frac{2RT}{E}\right] - \frac{E}{2.303RT} \ldots\ldots 1$$

In the analysis formula, the terms Wf and Wt stand for the quantity of mass lost at the conclusion of every phase and the weight that a certain temperature, respectively. E stands for the activating energy, and R stands for the gas constant, which is (8.314 J·mol^(-1)·K^(-1)) The pre-exponential number is written as A, and the rate of heating at 10 C/min is written as.

The slope and the intersection were used to figure out the numbers of E and A. Equations (2-4) were used to figure out the values of H, S, and G at each step.

$$\Delta H = \Delta E - RT \quad ----------(2)$$

$$\Delta S = R\ ln\left(Ah / KBTS\right) \quad -------(3)$$

$$\Delta G = \Delta H - T\Delta S \quad ----------(4)$$

The equations incorporate additional variables: h, which stands for Planck's constant (6.6262x10(-34) Js, and KB, which stands for Boltzmann's constant1.3806x10^(-23) J/K).. TS stands for the highest temperature. The results showed that the process of breakdown was endothermic, which was clear from the positive readings of H. The negative readings of S show that the organization of the complexes was higher than that of the reactants. Also, the positive numbers of G showed that the steps did not happen on their own. Figures 17, 18, and 19 back up these results, and studies [28, 29] have talked about them before.

Tab 4. Some thermodynamic functions of prepared compounds

Formula of complex	stage	E	ΔH	ΔS	ΔG
		KJ/mole	KJ/mole	KJ/mole	KJ/mole
LB	1	261.41	258.8	-158.32	309.24
LBMn	1	140.9	136.3	-172.43	232.14
	2	193.85	188.54	-171.36	297.82
LACo	1	107.78	104.13	-170.1	179.25
	2	152.75	148.4	-169.51	237.46
	3	231.36	225.1	-170.84	333.38
	4	247.3	241.63	-171.5	358.31

There are a variety of [LA Mn] were tested for their inhibitory effects on the growth of breast cancer cells (SK-GT-4) and healthy cells (HBL100) at concentrations ranging from 50 µg/ml to 1000 µg/ml. The viability of SK-GT-4 cells after treatment with Mn (II) complex is shown in Table (5). The highest inhibition ratio of SK-GT-4 cells was observed at a concentration of 750 µg/ml, reaching 97.44%. In comparison, the highest inhibition ratio of HBL100 cells was 18.63% at the same concentration. The IC50 value of the Mn (II) complex was determined to be 104 µg/ml (Figure 20).

A comparison between the cancerous cell line (SK-GT-4) and the normal cell line (HBL100) is shown in Figure 21. The results demonstrate that at a concentration of 750 µg/ml, [Mn LA] effectively kills more than half of the cancerous cells while having a lesser effect on healthy cells. These findings suggest that the Mn (II) complex has therapeutic potential as a treatment for cancer of the breast [30].

Fig 1. Mass Spectrum of the Ligand (A)

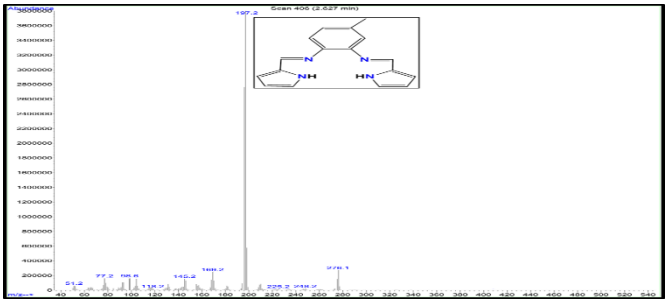

Fig 2. Mass Spectrum of the Ligand (B)

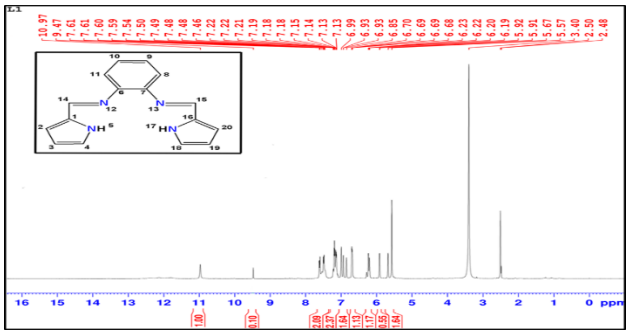

Fig 3. 1H NMR spectrum of the Ligand (A).

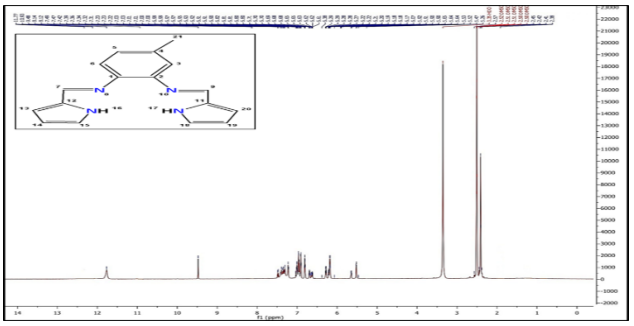

Fig 4. 1H NMR spectrum of the Ligand (B).

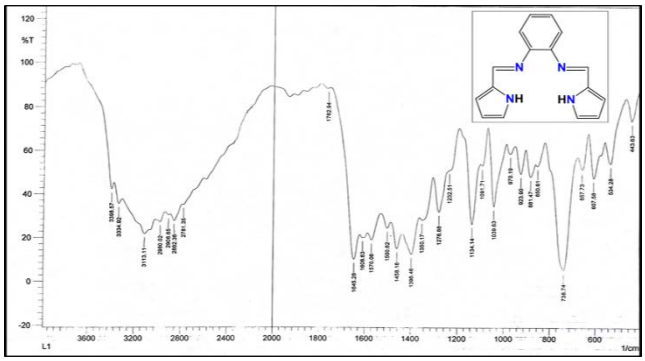

Fig 5. FT-IR spectrum of (LA)

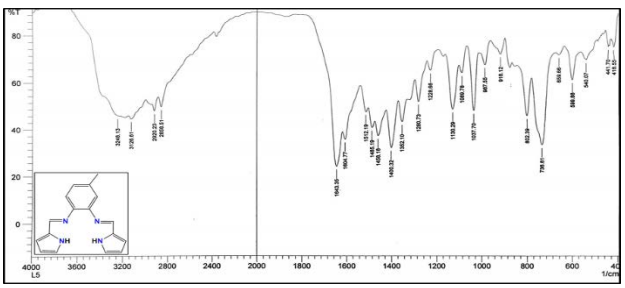

Fig 6. FT-IR spectrum of (LB)

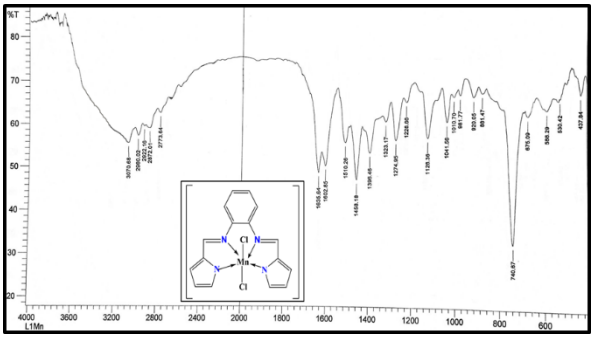

Fig 7. FT-IR spectrum of (MnLA)

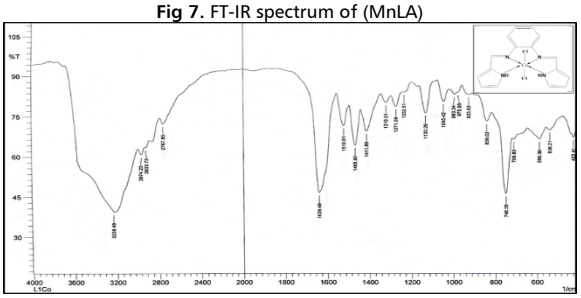

Fig 8. FT-IR spectrum of (CoLA)

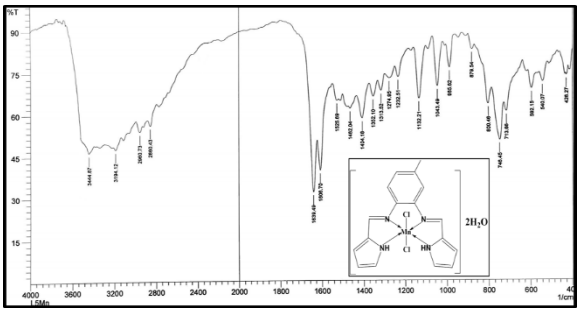

Fig 9. FT-IR spectrum of (MnLB)

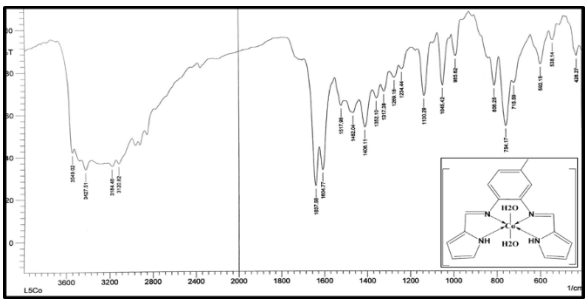

Fig 10. FT-IR spectrum of (CoLB)

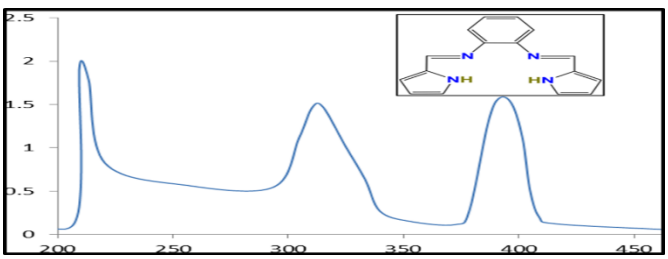

Fig 11. UV-Vis spectrum of (LA)

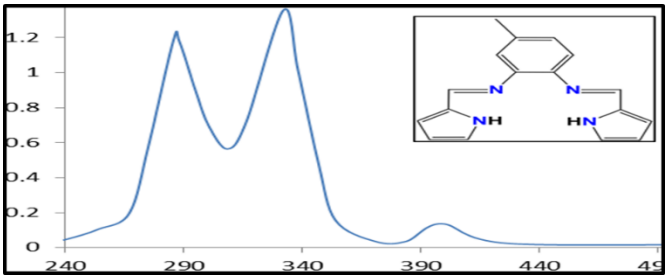

Fig 12. UV-Vis spectrum of (LB)

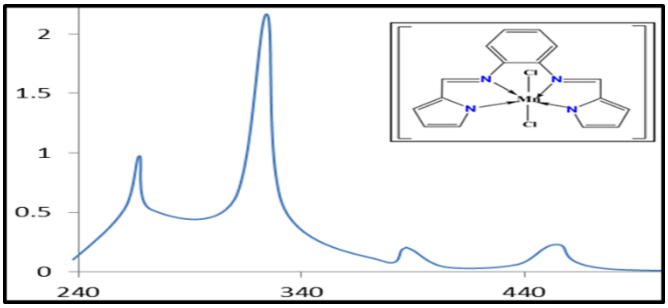

Fig 13. UV-Vis spectrum of (MnLA)

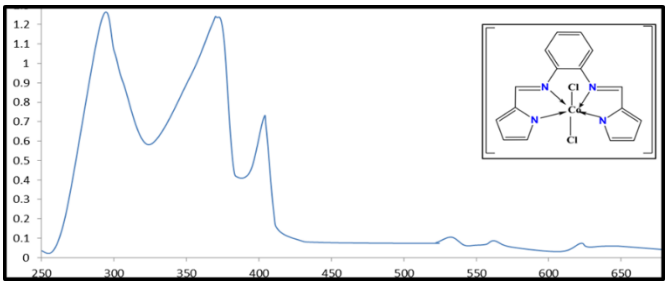

Fig 14. UV-Vis spectrum of (CoLA)

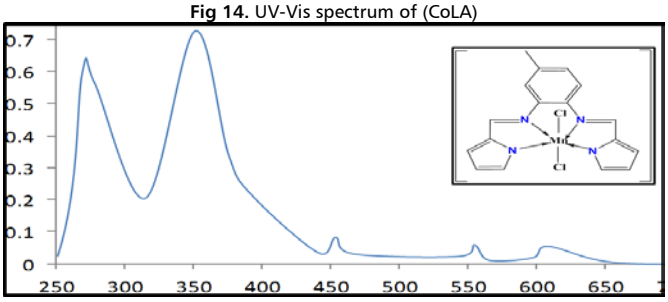

Fig 15. UV-Vis spectrum of (MnLB)

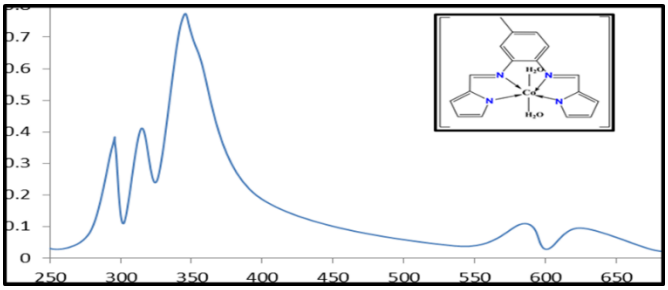

Fig 16. UV-Vis spectrum of (CoLB)

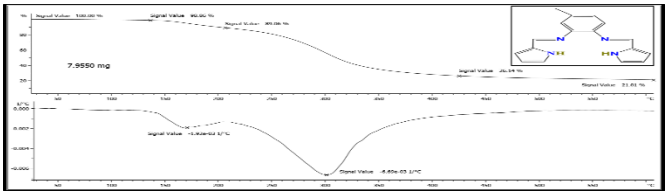

Fig 17. TG curve of (LB)

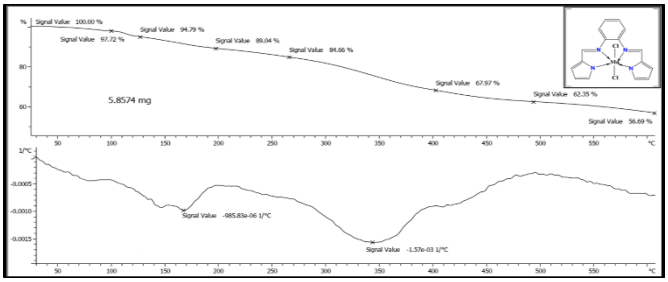

Fig 18. TG curve of (MnLA)

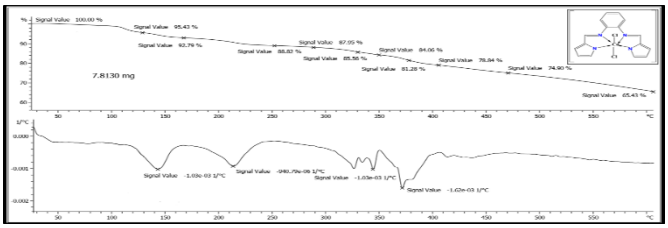

Fig 19. TG curve of (CoLA)

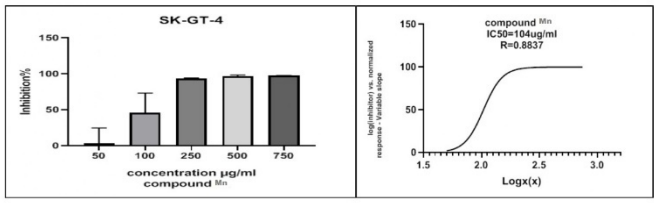

Fig 20. Rate viability of SK-GT-4 cell line treated with five replicates of concentrations(*µg*/ml) from Mn (II) complex with IC50 in *µg*/ml.

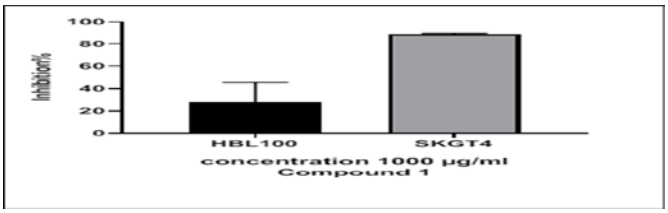

Fig 21. Comparison of an Cancerous line cells of (SK-GT-4) and Normal line cells of(HBL100)

Tab 5. Comparison of [Mn LA]'s effect on the viability of breast cancer cells (SK-GT-4) and normal cells (HBL100) after 24 hours in a 37 C0 MTT assay

Mean Percentage (%) for each cell line				Mn Con.
Normal line cells of(HBL100)		Cancerous line cells of (SK-GT-4)		(µg.mL−1)
Cell Inhibition	Cell Viability	Cell Inhibition	Cell Viability	
3.05	96.95	3.61	96.39	50
6.77	93.23	45.83	54.17	100
7.11	92.89	93.68	6.32	250
12.03	87.97	96.55	3.45	500
18.63	81.37	97.44	2.56	750
27.56	72.44	88.92	11.08	1000

CONCLUSION

Two novel metal complexes were produced using a binucleation ligand. Traditional analytical methods and a wide range of physicochemical techniques were used to conduct in-depth characterisation. The hypothesized structures of the compounds were verified by FTIR, electrical change, 1H NMR, and MAS investigations. Magnetic susceptibility and electric conductivity measurements provided additional evidence, indicating that complexes 1-5 possessed a distorted tetrahedral geometry.

In terms of biological activity, the Mn (II) complexes showed promising potential against cancer cells (SK-GT-4) in preliminary investigations. However, further studies are necessary to optimize and identify the most effective complex. Additional research can focus on refining the properties and activity of these complexes for potential applications in cancer treatment.

ACKNOWLEDGMENTS

The authors would like to offer their heartfelt thanks to the Principal and Management of the Tissue Culture Lab at Basrah University's College of Education for Pure Science. In addition, those involved with the Iraqi Council for Health and Disease Genetic Research would want to express their gratitude to the institute's administration.

REFERENCES

1. Sharma D, Revanasiddapp HD, Kumar BCV, Jayalakshmi B, et al. Co(III) and VO(IV) complexes with a new bidentate Schiff base: Interaction with BSA and antimicrobial studies. Biointerface Res Appl Chem. 2019;9:3776-3782.
2. Buldurun K, Turan N, Savci A, Colak N, et al. Synthesis, structural characterization and biological activities of metal(II) complexes with Schiff bases derived from 5-bromosalicylaldehyde: Ru(II) complexes transfer hydrogenation. J Saudi Chem Soc. 2019;23:205-214.
3. Hossain MS, Banu LA, E-Zahan MK. Synthesis, characterization and biological activity Bipyridine. Appl Sci Res Rev. 2019;6:2394-9988.
4. Slassi S, Tailler AF, Larcher G, Amine A, et al. Imidazole and Azo-Based Schiff bases ligands as Highly Active Antifungal and Antioxidant Components. Heteroatom Chem. 2019; Article ID 6862170: 8.
5. Mohammed NL, Al-Shawi JMS, Kadhim MJ. Synthesis, Characterization and Thermal Studies of Schiff Bases Derived from 2,4-Dihydroxy benzaldehyde and their Complexes with Co (II), Ni (II), Cu (II). Int J Sci Eng Res. 2019;7(1):31-40.
6. Valarmathy G, Subbalakshmi R, Rengathan R, Kokila R, et al. Synthesis of Schiff base (E)-2-(((3-Hydroxyphenyl)imino)methyl)-6-methoxyphenol Containing N and O Donors and its Metal Complexes: Spectral, Thermal, Redox Behaviour, Fluorescence Quenching, Antimicrobial and Anticancer Studies. Asian J Chem. 2018;30:645-650.
7. Wankhede BS, Patil AB. Studies on Ti(III), Cr(III) and Fe(III) complexes with 1-(1-hydroxynaphthalen-2-yl) ethanone-4-chloro benzoylhdrazone ligand: Synthesis, Physicochemical and Antimicrobial activity. J Pharm Chem Bio Sci. 2018;6:25-33.
8. Arumugam AP, Elango G, Guhanathan S, et al. Synthesis and Characterization of Novel Schiff base Cu(II) Complexes: Antimicrobial and Molecular Docking Studies. J Chem Environ Sci Appl. 2017;3:75-90.
9. Mohammadi K, Asadi M, Khah MS, Sepehrpour H, et al. Symmetrical and Unsymmetrical Schiff bases Derived from 3,4-Diaminobenzophenone, Synthesis and thermodynamics of five Coordinated Tertiaryphosphine Cobalt(III) Complexes. Croat Chem Acta. 2016;89:277-284.
10. Yassin SK, Alshawi JM, Salih ZAM. Egypt J Chem. 2020;63:4005-4016.
11. Yassin SK, Alshawi JM, Salih ZAM. Orient J Chem. 2020;36:940-945.
12. Tokala R, Bale S, Janrao IP, et al. Synthesis of 1,2,4-triazole-linked urea/thiourea conjugates as cytotoxic and apoptosis inducing agents. Bioorg Med Chem Lett. 2018;28(10):1919-1924.
13. Tsednee M, Huang YC, Chen YR, Yeh KC. Identification of metal species by ESIMS/MS through release of free metals from the corresponding metal-ligand complexes. Sci Rep. 2016;6(1):26785.
14. Kamakshi R, Reddy BSR. Synthesis of chalcone-based fluorescent polymers: Diels-Alder reaction of chalcones and their polymerization through ROMP. J Polym Sci Part A: Polym Chem. 2008;46:1521-1531.
15. Kadhum MY, Abduljleel AM. Synthesis, characterization and biological studies of Schiff bases derived from piperonal and their complexes with cobalt (II). Der Pharma Chemica. 2014;6(5):88-100.
16. Meghdadi S, Amirnasr M, Mereiter K, Molaee H, Amiri A, et al. Synthesis, structure and electrochemistry of Co(III) complexes with an unsymmetrical Schiff base ligand derived from 2-aminobenzylamine and pyrrole-2-carboxaldehyde. Polyhedron. 2011;30(10):1651-1656.
17. Mir JM, Rajak DK, Maurya RC. Oxovanadium (IV) complex of 8-hydroxy quinoline and 3-acetyl-6-methyl-2H-pyran-2, 4 (3H)-dione: Experimental, theoretical and antibacterial evaluation. J King Saud Univ Sci. 2019;31(4):1034-1041.
18. Hadi MA, Kareem IK. Synthesis, characterization and spectral studies of a new Azo-Schiff base ligand derived from 3,4-diamino benzophenone and its complexes with selected metal ions. Res J Adv Sci. 1(1):54-73.
19. El-Ghamry HA, Gaber M, Farghaly TA. Mini reviews in medicinal chemistry. 2019;19(13):1068-1079.
20. Aliyu HNA, Ado I. Biosci Res Commun. 2009;21(5):215-220.
21. Powers IG, Andjaba JM, Luo X, Mei J, Uyeda C. J Am Chem Soc. 2018;140(11):4110–4118.
22. Anacona J, Santaella J. Molecular and Biomolecular Spectroscopy. 2013;115:800-804.
23. Ur-Rehman S, Ikram M, Rehman S, Jan N. J Mex Chem Soc. 2011;55(3):164-167.
24. Abass SK, A-Hilfi JA, Abbas SK, Ahmed LM. Indones J Chem. 2020;20(2):404-412.
25. G, S, M, A. Chem Commun. 2015;51:9169-9172.
26. J.Pait A, K.J Donde, S.S Raut, V.R Pait, R.S Lokhande. J Chem Pharm Res. 2012;4(2):1413-1425.
27. Hadi JS, Abdulnabi ZA, Dhumed AM. European Journal of chemistry. 2017;8(3):252-257.
28. J Venkatesan, M Sekar, V Thonikcchalam, G Manikandan. Der Pharma Chemica. 2017;9(14):164–197.
29. Shalan N, Balkhi AM, Hamo S, fALAH A. J of AlNahrain university. 2014;17(3):1-8.
30. Refat, Moamen S., et al. "Synthesis, physicochemical characterization and anticancer screening of sulfa drug ruthenium complexes as anticancer agent." J Mol Liquids. 2016;222:334-349.